Journal of Alloys and Compounds 509 (2011) 2964–2969

Contents lists available at ScienceDirect

Journal of Alloys and Compounds

journal homepage: www.elsevier.com/locate/jallcom

Properties and fast low-temperature consolidation of nanocrystalline Ni–ZrO_2 composites by high-frequency induction heated sintering

In-Jin Shon*, Hyun-Su Kang

Division of Advanced Materials Engineering, Research Center of Advanced Materials Development, Chonbuk National University, Jeonbuk 561-756, Republic of Korea

ARTICLE INFO

Article history:
Received 7 October 2010
Received in revised form
13 November 2010
Accepted 19 November 2010
Available online 1 December 2010

Keywords:
Composite
Chemical synthesis
Nanostructures
Sintering

ABSTRACT

Nanopowders of Ni and ZrO_2 (11 nm and 90 nm, respectively) were synthesized from NiO and Zr by high energy ball milling. A highly dense nanostructured 2Ni–ZrO_2 composite was consolidated at low temperature by high-frequency induction heat sintering within 2 min of the mechanical synthesis of the powders (Ni–ZrO_2) with horizontal milled NiO + Zr powders under 500 MPa pressure. This process allows very quick densification to near theoretical density and prohibits grain growth in nano-structured materials. The grain sizes of Ni and ZrO_2 in the composite were calculated. Finally, the average hardness and fracture toughness values of nanostructured 2Ni–ZrO_2 composites were investigated.

1. Introduction

A continuous increase in the performance requirements of materials for aerospace and automotive applications has lead to the development of several structural composite materials. Among these, metal matrix composites refer to materials in which rigid ceramic reinforcements are embedded in ductile metal or alloy matrixes. Metal matrix composites combine metallic properties (ductility and toughness) with ceramic characteristics (high strength and modulus), leading to greater strength in shear and compression and to higher service temperature capabilities. The attractive physical and mechanical properties that can be obtained with metal matrix composites, such as high specific modulus, strength-to weigh ratio, fatigue strength, temperature stability and wear resistance, have been documented extensively [1].

ZrO_2 has a density of 5.98 g cm^{-3}, a Young's modulus of 210 GPa, excellent oxidation resistance and good high-temperature mechanical properties [2]. Ni has a density of 8.908 g cm^{-3}, a Young's modulus of 200 GPa and good fracture toughness [3]. Hence, a composite consisting of Ni and ZrO_2 may be able to provide the mechanical property requirements of a superior structural material.

Nanocrystalline materials have potential as advanced engineering materials with improved physical and mechanical properties [4,5]. Recently, nanocrystalline powders have been developed by thermochemical and thermomechanical processes such as the spray conversion process (SCP), co-precipitation, high energy milling and electrical wire explosion [6–9]. However, the grain sizes of sintered materials are much larger than those of pre-sintered powders due to rapid grain growth that occurs during conventional sintering. Controlling grain growth during sintering is a key to the commercial success of nanostructured materials. Unconventional sintering techniques, including high-pressure densification, magnetic pulse compaction and shock densification, have been proposed to overcome the problem of grain growth [10–12]. However, these methods have failed to provide fast, reproducible techniques that yield large quantities of high density samples with nanostructured grains.

The high-frequency induction heated sintering (HFIHS) method recently emerged as an effective technique for sintering and consolidating high temperature materials [13,14]. HFIHS is similar to traditional hot-pressing, but the sample is heated by an induced electric current that flows through the sample and a die. This process increases the heating rate (up to 1000 °C/min) to a degree much higher than that of traditional hot-press sintering.

The purpose of this work is to produce nanopowders of Ni, ZrO_2 and dense nanocrystalline 2Ni–ZrO_2 composites. In our technique, composites are formed within 2 min of the mechanical synthesis of the powders (Ni–ZrO_2) and horizontal milled 2NiO + Zr powders using the induced current activated sintering method. Further, we evaluate the grain size and mechanical properties (hardness and fracture toughness) of the resulting materials.

* Corresponding author. Tel.: +82 63 2381; fax: +82 63 270 2386.
E-mail address: ijshon@chonbuk.ac.kr (I.-J. Shon).

0925-8388/$ – see front matter © 2010 Elsevier B.V. All rights reserved.
doi:10.1016/j.jallcom.2010.11.170

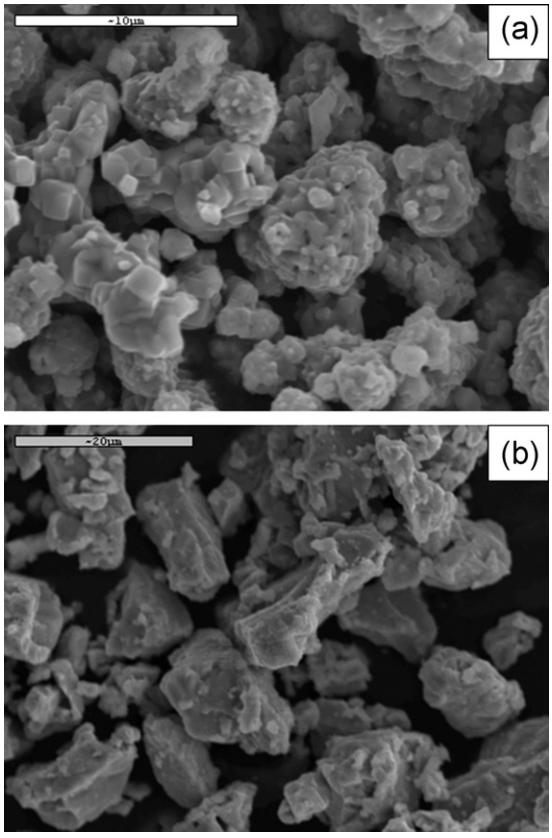

Fig. 1. Scanning electron microscope image of raw materials: (a) NiO and (b) Zr.

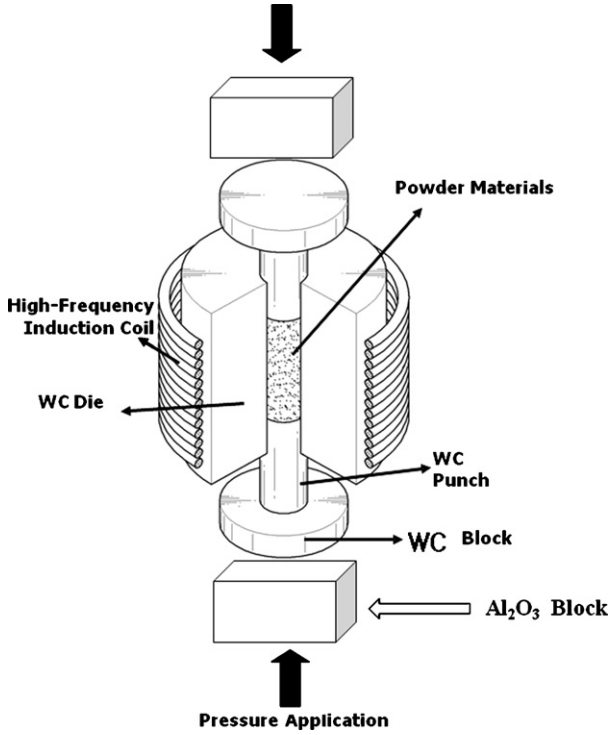

Fig. 2. Schematic diagram of the high-frequency induction heated sintering apparatus.

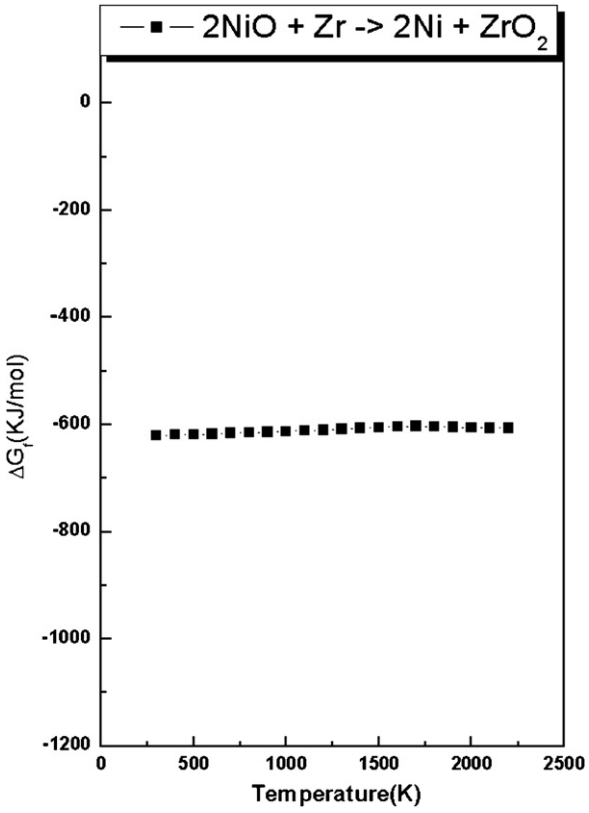

Fig. 3. Temperature dependence of the Gibbs free energy variation by interaction of NiO with Zr.

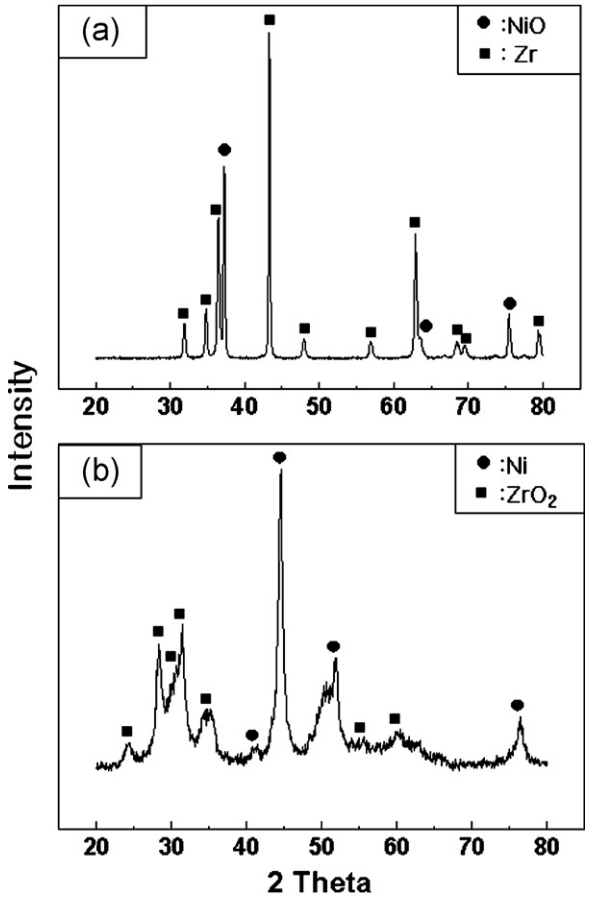

Fig. 4. XRD patterns of the milled powder by (a) horizontally milling and (b) mechanically milling.

2. Experimental procedures

Powders of 99.5% NiO (<325 mesh, Alfa, Aesar, USA) and 99.5% pure Zr (-325 mesh, Sejong Materials Co., LTD, Korea) were used as starting materials. The NiO powder and Zr powder have round and irregular grain shapes, respectively, as shown in Fig. 1. NiO and Zr powders with molar ratio of 2:1 were mixed by two types of methods. First, the powders were milled in a high-energy ball mill, i.e., a Pulverisette-5 planetary mill, at 250 rpm and for 10 h. Tungsten carbide balls (8.5 mm in diameter) were used in a sealed cylindrical stainless steel vial under an argon atmosphere. The weight ratio of ball-to-powder was 30:1. Second, the powders were mixed in polyethylene bottles using zirconia balls with ethanol and were milled at a horizontal rotation velocity of 250 rpm for 10 h. The crystallite sizes of Ni and ZrO_2 were calculated by the formula suggested by Suryanarayana and Grant Norton [15]:

$$B_r(B_{crystalline} + B_{strain})\cos\theta = \frac{k\lambda}{L} + \eta\sin\theta \quad (1)$$

where B_r is the full width at half-maximum (FWHM) of the diffraction peak after instrument correction, $B_{crystalline}$ and B_{strain} are the FWHM caused by small crystallite size and internal stress, respectively, k is constant (with a value of 0.9), λ is the wavelength of the X-ray radiation, L and η are the crystallite size and internal strain, respectively, and θ is the Bragg angle. The parameters B and B_r follow Cauchy's form with the relationship: $B = B_r + B_s$, where B and B_s are the FWHM of the broadened Bragg peaks and the standard sample's Bragg peaks, respectively.

After milling, the mixed powders were placed in a WC die (outside diameter, 40 mm; inside diameter, 5 mm; height, 40 mm) and then introduced into the high-frequency induction heated sintering system made by Eltek in South Korea, shown schematically in Fig. 2. The four major stages in the synthesis are as follows. The system was evacuated (stage 1). Next, a uniaxial pressure of 500 MPa was applied (stage 2). A induced current was then activated and maintained to 650 °C with a heating rate of 600 °C/min and was then turned off without a holding time (stage 3). At the end of the process, the sample was cooled to room temperature (stage 4). The process was carried out under a vacuum of 40 mTorr.

The relative densities of the sintered samples were measured by the Archimedes method. Microstructural information was obtained from polished product samples. Compositional and micro structural analyses of the products were made through X-ray diffraction (XRD) and scanning electron microscopy (SEM) with energy dispersive X-ray analysis (EDAX). Vickers hardness was measured by performing indentations at a load of 10 kg and a dwell time of 15 s on the synthesized samples.

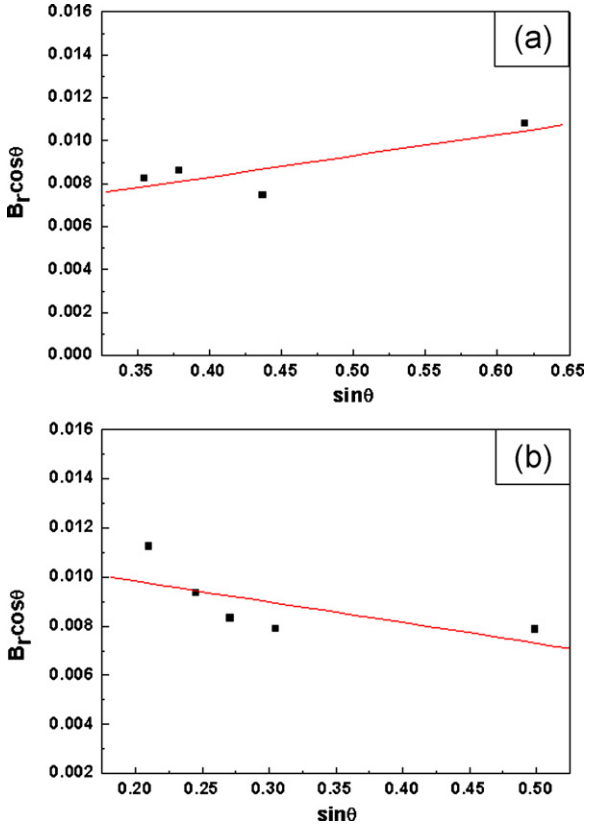

Fig. 5. Plot of $B_r\cos\theta$ versus $\sin\theta$ of Ni (a) and ZrO_2 (b) in high energy ball milled powders.

3. Results and discussion

The interaction between NiO and Zr:

$$2NiO + Zr \rightarrow 2Ni + ZrO_2 \quad (2)$$

is thermodynamically feasible, as shown in Fig. 3.

The X-ray diffraction pattern of horizontal milled powder and mechanically high energy ball milled powders from raw powders is shown in Fig. 4(a) and (b), respectively. Ni–ZrO_2 was not synthesized during the horizontal rotation ball milling in ethanol, but synthesized during high energy ball milling. From the above results,

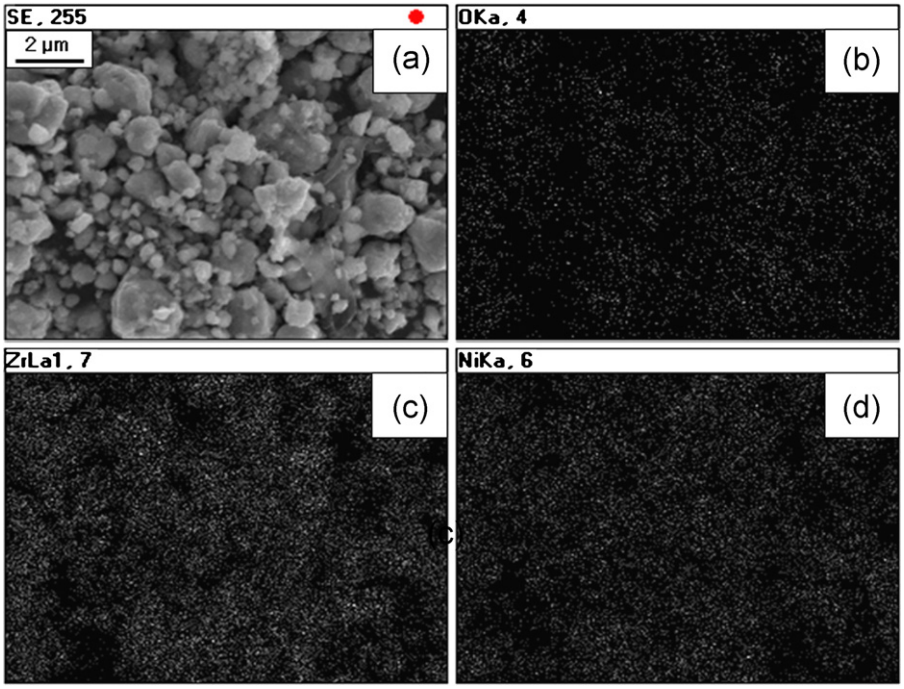

Fig. 6. SEM image, X-ray mapping and EDS of high energy ball milled powders of NiO–Zr.

the solid replacement reaction is completed during high energy ball milling. The full width at half-maximum (FWHM) of the diffraction peak is broad due to refinement of the powder and strain. Fig. 5 shows a plot of $B_r \cos\theta$ versus $\sin\theta$ used to calculate crystallite size of Ni and ZrO_2 in high energy ball milled powders. The average crystallite sizes of ZrO_2 and Ni obtained from Eq. (1) were about 12 nm and 31 nm, respectively. Fig. 6 shows an SEM image, X-ray mapping and EDS of the high-energy ball milled powder of 2NiO–Zr. From the SEM image, the powders are agglomerated, while X-ray mapping at same point shows that Zr and O are detected. Further, O, Zr and Ni peaks are detected in EDS.

An XRD pattern of the Ni–ZrO_2 composite heated to 650 °C is shown in Fig. 7. Only Ni and ZrO_2 peaks are detected. Based on the X-ray patterns of Fig. 4(a) and Fig. 6(b), Ni–ZrO_2 was synthesized from horizontal milled powder of 2NiO and Zr during heating. Fig. 8 shows a plot of $B_r \cos\theta$ versus $\sin\theta$, again used to calculate the crystallite size of Ni and ZrO_2. The structure parameters, i.e., the average crystallite sizes of Ni and ZrO_2, are 64 and 34 nm and 46 and 26 nm, respectively. Further, the relative density of the Ni–ZrO_2 composites were 97% and 96%, respectively. FE-SEM images of Ni–ZrO_2 composites sintered at 650 °C from horizontal milled powders and high energy ball milled powders are shown in Fig. 9. As shown, the composites consist of nano-crystallites.

Composites made up of nano-crystallites and high Ni–ZrO_2 densities were obtained at low temperatures for two reasons. First, the small crystallite size is attributed to the high heating rate and relatively short powder exposure to high temperature. The types of current (resistive or inductive) used in sintering and/or synthesis have been the focus of several attempts to explain enhanced sintering and improved product characteristics. The role of current is explained in terms of fast Joule heating, the presence of plasma in pores separating powder particles, and the intrinsic contribution of

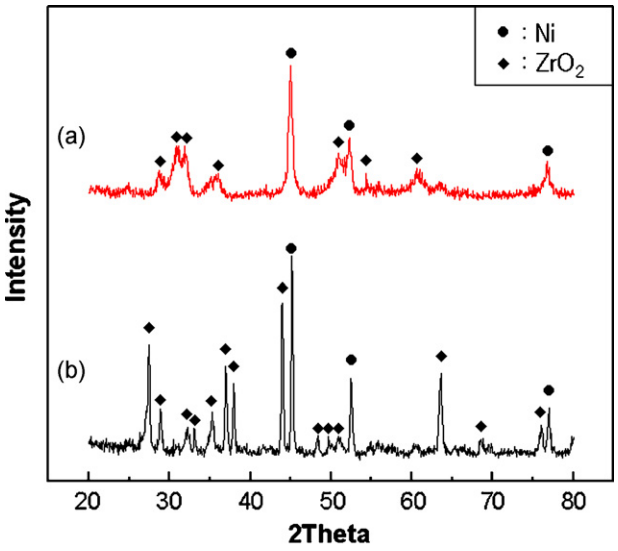

Fig. 7. XRD patterns of Ni–ZrO_2 composite sintered from (a) high energy ball milled powders and (b) horizontal milled powders.

current to mass transport [16–19]. Second, applying pressure during initial sintering adds another term to the surface energy driving force such that the total driving force, F_D, may be expressed as [20]:

$$F_D = \gamma + \left(\frac{P_a r}{\pi}\right) \quad (3)$$

where γ is the surface energy, P_a is the applied pressure, and r is the particle radius. The effect of pressure on the densification of nanometric, stabilized ZrO_2 during high frequency-induced heated

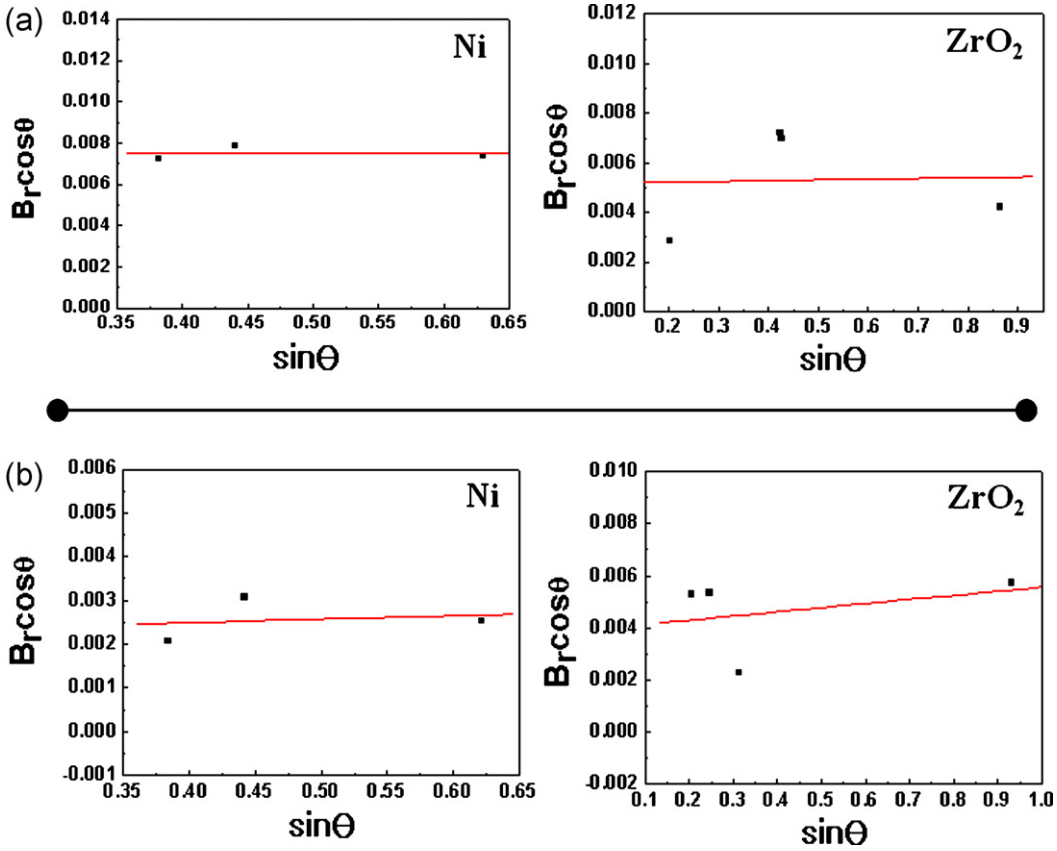

Fig. 8. Plot of $B_r \cos\theta$ versus $\sin\theta$ of Fe and ZrO_2 composites sintered from (a) high energy ball milled powders and (b) horizontal milled powders.

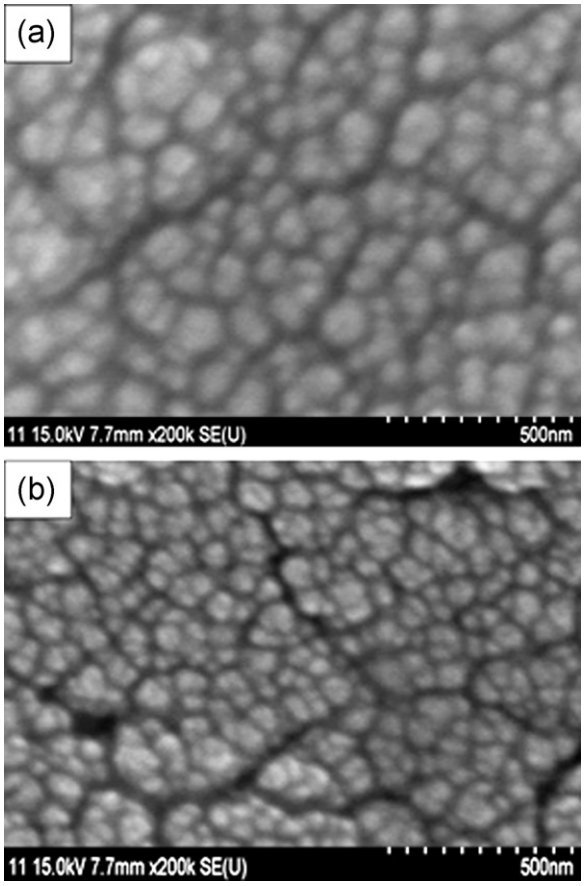

Fig. 9. FE-SEM images of Ni–ZrO_2 composite sintered from (a) horizontal milled powders and (b) high energy ball milled powders.

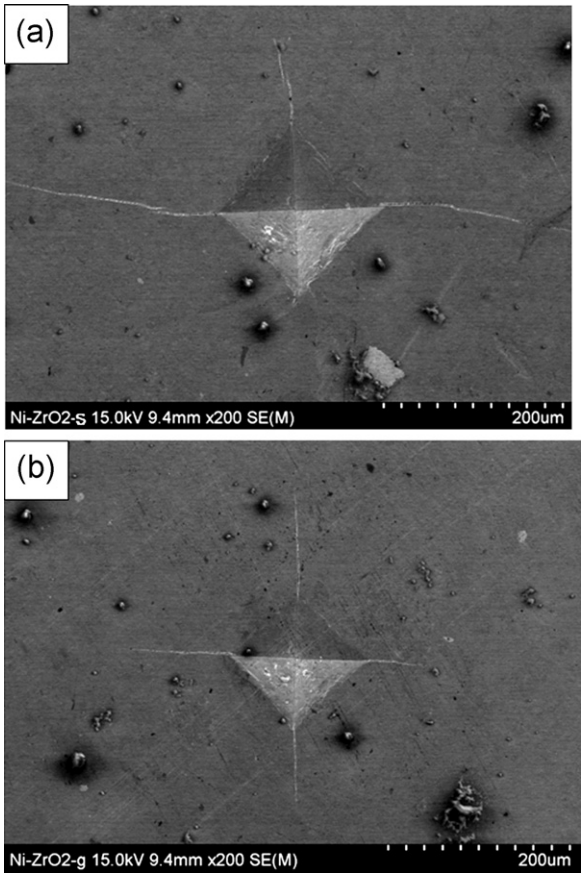

Fig. 10. Vickers indentation in the Ni–ZrO_2 composite sintered from (a) horizontal milled powders and (b) high energy ball milled powders.

sintering was investigated by Shon et al. [21]. The relative density increased significantly as pressure increased from 60 to 100 MPa for sintering at 1000 °C.

Vickers hardness measurements were made on polished sections of the Ni–ZrO_2 composite using a 10 kg_f load and 15 s dwell time. The hardness values of the Ni–ZrO_2 composite sintered at 650 °C from horizontal milled powders and high energy ball milled powders were calculated as 650 and 760 kg/mm^2, respectively. These values represent an average of five measurements each. Indentations with large enough loads produced median cracks around the indent. The length of these cracks permits an estimation of the fracture toughness of the material. From the length of these cracks, fracture toughness values can be determined using the equation suggested by Anstis et al. [22]:

$$K_{IC} = 0.016\left(\frac{E}{F}\right)^{1/2}\left(\frac{P}{C}\right)^{3/2} \quad (4)$$

where E is the Young's modulus, H the indentation hardness, P the indentation load, and C the trace length of the crack measured from the center of the indentation. The modulus was estimated by the rule mixtures for a 0.39 volume fraction of ZrO_2 and 0.61 volume fraction of Ni using $E(ZrO_2) = 210$ GPa [2] and $E(Ni) = 211$ GPa [3]. As in the cases of the hardness values, the toughness values were derived by averaging five measurements. The toughness values of composites obtained from horizontal milled powders and high energy ball milled powders are 9 and 10 MPa m$^{1/2}$, respectively.

The hardness and fracture toughness of ZrO_2 are reported as 11.8 GPa and 6.5 MPa m$^{1/2}$, respectively [23]. The hardness of the Ni–ZrO_2 composite is lower than that of monolithic ZrO_2 but the fracture toughness is higher than that of ZrO_2 due to the addition of ductile Ni. Fig. 10 shows Vickers indentations in the Ni–ZrO_2 composite sintered from (a) horizontal milled powders and (b) high energy ball milled powders. One to three additional cracks were observed to propagate from the indentation corner.

4. Conclusions

Nanopowders of ZrO_2 and Ni were synthesized from Zr and NiO by high energy ball milling. The powder sizes of Ni and ZrO_2 were 31 nm and 12 nm, respectively. Using the high-frequency induction heated sintering method, the densification of nanostructured Ni–ZrO_2 composite was accomplished using mechanically synthesized powders and horizontal milled powders within 2 min of synthesis. The average crystallite sizes of Ni and ZrO_2 prepared by HFIHS were lower than 100 nm. The average hardness and fracture toughness values obtained from mechanically synthesized powders and horizontal milled powders were 760 and 650 kg/mm^2 and 10 and 9 MPa m$^{1/2}$, respectively. The fracture toughness of the Ni–ZrO_2 composite is higher than that of monolithic ZrO_2.

Acknowledgment

This paper was supported by research funds of Chonbuk National University in 2010.

References

[1] L. Ceschini, G. Minak, A. Morri, Compos. Sci. Technol. 66 (2006) 333–340.
[2] S.G. Huang, J. Eur. Ceram. Soc. 27 (2007) 3269–3275.
[3] http://en.wikipedia.org/wiki/Elastic_properties_of_the_elements (data page).
[4] M.S. El-Eskandarany, J. Alloys Compd. 305 (2000) 225–238.
[5] L. Fu, L.H. Cao, Y.S. Fan, Scripta Mater. 44 (2001) 1061–1068.

[6] Z. Fang, J.W. Eason, Int. J. Refract. Met. Hard Mater. 13 (1995) 297–303.
[7] A.I.Y. Tok, l.h. Luo, F.Y.C. Boey, Mater. Sci. Eng. A 383 (2004) 229–234.
[8] I.J. Shon, D.K. Kim, K.T. Lee, K.S. Nam, Met. Mater. Int. 14 (2008) 593–598.
[9] W. Kim, J.S. Park, C.Y. Suh, S.W. Chon, S.L.I.J. Shon, Mater. Trans. 50 (2009) 2897–2899.
[10] S.C. Liao, W.E. Mayo, K.D. Pae, Acta Mater. 45 (1997) 4027–4032.
[11] Z.Q. Jin, C. Rockett, J.P. Liu, K. Hokamoto, N.N. Thadhani, Mater. Sci. Forum 465–466 (2004) 93–97.
[12] V. Ivanov, S. Paranin, V. Khrustov, A. Medvedev, A. Shtol'ts, Key Eng. Mater. 206–213 (2002) 377–381.
[13] H.C. Kim, I.J. Shon, J.K. Yoon, J.M. Doh, Met. Mater. Int. 12 (2006) 141–147.
[14] H.C. Kim, I.J. Shon, I.K. Jeong, I.Y. Ko, Met. Mater. Int. 12 (2006) 393–398.
[15] C. Suryanarayana, M. Grant Norton, X-ray Diffraction: A Practical Approach, Plenum Press, New York, 1998.
[16] Z. Shen, M. Johnsson, Z. Zhao, M. Nygren, J. Am. Ceram. Soc. 85 (2002) 1921–1927.
[17] J.E. Garay, U. Anselmi-Tamburini, Z.A. Munir, S.C. Glade, P. Asoka-Kumar, Appl. Phys. Lett. 85 (2004) 573–575.
[18] J.R. Friedman, J.E. Garay, U. Anselmi-Tamburini, Z.A. Munir, Intermetallics 12 (2004) 589–597.
[19] J.E. Garay, U. Anselmi-Tamburini, Z.A. Munir, Acta Mater. 51 (2003) 4487–4495.
[20] R.L. Coble, J. Appl. Phys. 41 (1970) 4798–4802.
[21] Hwan-Cheol, In-Jin Shon, In-Kyoon Jeong, In-Yong Ko, Met. Mater. Int. 12 (2006) 393–398.
[22] G.R. Anstis, P. Chantikul, B.R. Lawn, D.B. Marshall, J. Am. Ceram. Soc. 64 (1981) 533–543.
[23] S.G. Huang, K. Vanmeensel, O. Van der Biest, J. Vleugels, J. Eur. Ceram. Soc. 27 (2007) 3269–3275.